Journal of Additive Manufacturing Technologies
DOI: 10.18416/JAMTECH.2111530

Infinite Science | Publishing

Parametric simulations for residual stresses and distortions of Inconel 625 fabricated by laser powder bed fusion additive manufacturing

Ö. Poyraz[1], E. Yasa[2*], L.T. Tunç[3] and K. Kılıçay[2]

[1] *Department of Mechanical Engineering, Eskişehir Technical University, Eskişehir, Turkey*
[2] *Department of Mechanical Engineering, Eskişehir Osmangazi University, Eskişehir, Turkey*
[3] *Faculty of Engineering and Natural Sciences, Sabancı University, İstanbul, turkey*
[*] *Corresponding author, email:ozgurpoyraz@eskisehir.edu.tr*

Abstract

Developments related to the laser powder bed fusion (L-PBF) expanded the application area of the additive manufacturing (AM) for metal alloys, and increased the variety of machines and materials. On the other hand, this increase exposed the need for process development to adapt new materials and shapes with acceptable metallurgical, mechanical and geometrical attributes. In recent years, researchers have sought to reduce the development costs by decreasing these process development needs for some requirements. Among these, modeling and simulations for residual stresses and distortions are common practices. Dedicated software for these applications provided remarkable savings in computational times. Nevertheless, it is still necessary to pay attention to dedicated software, due to the fact that they might have some assumptions which are unknown to the end users. This study provides an in-depth investigation of Simufact Additive software based on L-PBF of Inconel 625 alloy. In this regard, thermo-mechanical simulations were performed by comparing the results with experimental data. Simulation set-ups were fine-tuned according to comparisons, and parametric analyses were conducted. The laser power and scanning speed were found to be the most influential parameters on the resulting residual stresses.

Keywords: Inconel 625, Laser powder bed fusion, Process parameters, Simufact Additive, Thermo-mechanical simulations

1. Introduction

Powder bed fusion (PBF) additive manufacturing (AM) is defined as the process in which regions of powders are fused selectively [1]. Laser or electron beam energy may be used to fully melt and fuse the metal powder particles [2]. Among these two processes, laser-based powder bed fusion (L-PBF) offers more variety in terms of nickel-based superalloys, which are of great importance for industries such as aerospace [3]. However, it is necessary to pay attention to the disadvantages that arise due to the application of immature L-PBF technology. Final product non-conformances, high raw material prices and high process development costs can be considered as some disadvantages. One of the widely observed phenomena in the macrostructure is the residual stresses and induced distortions.

Residual stresses, which reside inside the part following to L-PBF process, are cumulatively generated plastic strains as the result of cyclic thermal expansions and contractions. These stresses may cause distortions and possible process failure by recoater collisions, layer delamination or cracking [4]. Although there are many destructive and non-destructive techniques for measuring these residual stresses, parts could still be scrapped unless they conform to the requirements [5]. Furthermore, complying parts may still need post-processing in order to improve the dimensional accuracy of the distorted parts [6]. In this respect, it is preferable to predict and avoid these residual stresses.

Process modeling and simulation methods are widely employed and used to predict the residual stresses and distortions. Macro scale mechanical models are useful to predict Type I residual stresses, which vary over large distances and can be observed as deformations on the workpiece [4]. These macro scale simulations can be conducted on general purpose finite element method (FEM) software packages by coupling them with thermal models, but the computational time for such models, may take hundreds of hours to compute a 3-dimensional (3D) part with several layers [4]. In this context, dedicated process modeling and simulation software have been introduced especially for L-PBF. Amphyon, Ansys Additive, Autodesk Netfabb, Simufact Additive and Sunata can be sorted as examples to such software [7]. The dedicated software for L-PBF simulation reduces the computational times drastically, but the scientists or engineers using these software should pay attention while applying them. For example, it is seen that a previous researcher who has examined the thermo-mechanical or inherent strain methods used by many of these dedicated software has reported

problems and limitations for both methods [17]. The accuracy and uncertainty issues of thermo-mechanical simulations were highlighted together with the prediction errors of inherent strain method for the geometries rather than the calibration part [17]. On the other hand, if the two mentioned methods are applied correctly, they can be used in many useful tasks such as part-scale build orientation optimization [18]. In this respect, users shall benefit of the in-depth understanding of the principles of these software in order to achieve more realistic predictions. With this aim, scientists and engineers conduct research studies and benchmark various subjects such as software brand, part geometry, support structures and heat treatments [7-10].

This study presents a comprehensive investigation on the thermo-mechanical modeling with Simufact Additive Software, which is also used as an add-on with Materialise Magic software being the most common job preparation tool for L-PBF. In this regard, Inconel 625 was selected as the part material and both residual stresses and distortions were benchmarked with authors' previous experimental studies from the literature [5, 14]. Later on, voxel sensitivity studies were conducted and simulation set-ups were fine-tuned according to comparisons. Subsequently, parametric analyses were carried-out for energy input parameters as laser power, layer thickness, scan speed and hatch distance. Additionally, the influence of part dimensions and scanning strategy were examined. Achieved results were presented and the effects of examined subjects were discussed.

2. Material and methods

2.1. Material

In the scope of the study, Inconel 625 was selected as the part material with a wide application area in aerospace and aeroengine industry, and is commonly used for various components such as combustor liners, control housings and engine exhaust system. It possesses desirable service attributes such as high temperature strength together with resistance to oxidation, corrosion and pitting [11]. Further advantages of the selected material can be listed as having a specific and international L-PBF processing standard and also commercial powder availability among many machine and powder manufacturers [12]. The essential physical, thermal and mechanical properties of Inconel 625 used for the current study were derived from Simufact Additive software material database, and are presented in Table 1. Additional to the presented material properties, solidus temperature is taken as 1290°C whereas the melting temperature is considered as 1350°C. The stress-strain flow curves of the material were also considered for simulations.

2.2. Modeling

Simufact Additive is dominantly used for L-PBF, and it offers meso- and macro-scale simulation options. With the application of reasonably fast meso-scale simulations, thermal, mechanical or thermo-mechanically coupled problems can be solved. As a result, temperature history, displacements (distortions) and stresses can be predicted. On the other hand, extremely fast macro-scale simulations use inherent strain method and they analyze the process assuming it as a pure mechanical problem [13]. Considering the fact that thermal process parameters can only be adjusted in thermo-mechanical option, parametric simulations of this study were conducted using thermo-mechanical solver.

Table 1. Inconel 625 properties (Derived from Simufact Additive database)

Material Property (°C)	50	400	600
Density (kg/m^3)	8440 (constant)		
Specific Heat Capacity (J/g.K)	0.41 (constant)		
Thermal Conductivity (W/m.K)	11	15.5	18.5
Elastic Modulus (GPa)	205	185	175
Poisson Ratio (-)	0.28	0.30	0.31
Yield Strength (MPa)	725 (constant)		
Tensile Strength (MPa)	990 (constant)		

2.3. Process parameters and experimental studies

In order to benchmark the simulations with real life experiments, two different studies were selected from previous literature which use identical material and process parameters [5, 14]. In the first study by Kundakçıoğlu 2019, two rectangular cuboids were produced by L-PBF of Inconel 625 material, and the dimensions of the cuboid are 50 mm (X) by 10 mm (Y) by 7 mm (Z) [14]. After detaching from the base plate, the tip deflections of the cuboids were measured with co-ordinate measuring machines (CMM) and reported as 0.432 mm in one cuboid and 0.438 mm in the other one. In the second study by Yasa and Poyraz 2021, a rectangular cuboid was produced by L-PBF of Inconel 625 material, and the dimensions of the cuboid are 50 mm (X) by 50 mm (Y) by 10 mm (Z) [5]. After detaching from the base plate, micro indentation residual stress measurement technique was applied on the top surface of the specimen and the stress values of three discrete points are 123 MPa, 134 MPa and 149 MPa [5]. The process parameters used in the references studies are 285 W laser power, 0.040 mm layer thickness, 960 mm/s scanning speed and 0.1 mm hatch distance [5, 14]. Laser focus diameter was 0.1 mm and alternating scanning was used as the scanning strategy.

Within the scope of this study, it is aimed to compare the experimental results of the distortion sample, where the measurement region is more clearly defined, with the modeling results. Abovementioned process parameters were used and initial thermo-mechanical simulations were conducted on a computer with 4 cores, 2.40 GHz CPU and 16 GB RAM. The base plate

material was selected as C45 steel and its dimensions were considered as 250 mm (X) by 250 mm (Y) by 25 mm (Z).

Voxel-based surface mesh, representing a regular grid in 3D space, were used for finite element discretization. 3.5 mm was selected as the initial voxel size with the aim of achieving at least two voxel element representation for the smallest side (7 mm) of the distortion experiment cuboid. Although the simulation time was remarkably short, the convergence of the simulations to the experimental results was not acceptable. The simulations resulted in 0.54 mm tip deflection (displacement) where the average value of physical experiments was 0.43 mm (Fig 1a). This result exposed the need for smaller voxel sizes. In order to overcome this issue while maintaining reasonable computation times, voxel size sensitivity analysis was conducted. For this reason, voxel size was decreased to half of the one used for the previous attempt. As a result, 3.5 mm, 1.75 mm, 0.87 mm, 0.43 mm and 0.22 mm were used as voxel size magnitudes. The simulation results obtained using the 0.87 mm voxel size were 0.452 mm. Considering the experimentally obtained mean result of 0.435 mm, an acceptable level of 3.9% convergence was achieved. As seen from Fig. 1b, further voxel size decrease did not greatly influence the displacement results. This detected voxel size (0.87 mm) was also used in residual stress simulations and it was found to give an acceptable convergence with previous experimental studies [5]. As a result, this size was considered as the base for subsequent parametric simulations.

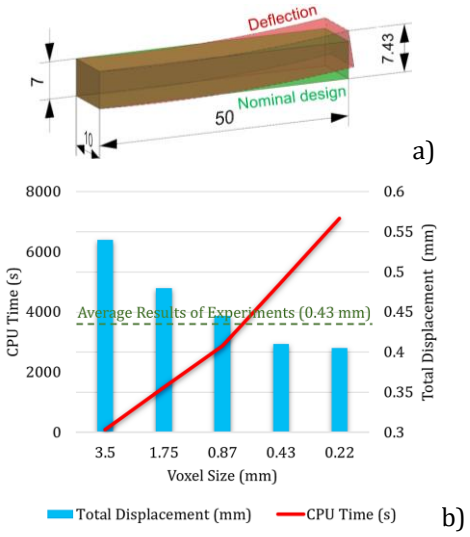

Fig 1. a) Comparison of nominal and deflected part after physical experiments b) Sensitivity study plot considering voxel size, total displacement and CPU time.

2.4. Parametric simulations

Previous process modeling and simulation efforts were considered during the planning stage of parametric simulations [9, 10, 15]. In a study conducted on a bridge geometry of Inconel 718 material [10], the effects of scanning strategies were benchmarked, and after removal from the base plate, residual stresses were reported as 1048 MPa for unidirectional scanning, and 1048 MPa for chessboard scanning. In another study conducted on a hexahedron geometry of Inconel 718 material [9], effects of scan interval for a constant scanning path were benchmarked, and effective residual stresses were reported as 296 MPa for 0.03 mm scan interval, 296 MPa for 0.09 mm scan interval and 296.5 MPa for 0.15 mm scan interval. Seeing that scanning strategies have inconsiderable effect on residual stresses, especially for simple geometrical shapes, they were excluded from the parametric simulation plans. Furthermore, previous researchers [9, 10, 15] investigated extremely high parameter level changes such as the use of scanning speed levels of 300 mm/s, 600 mm/s and 900 mm/s in the same benchmark. However, these alterations may not be possible in real cases since they may influence other attributes like residual porosity in the part. For this reason, parameter changes in this study were limited to 10% increments and parametric simulations were carried out with two increment steps in the up and down directions for each of the parameters, taking the ones verified by experiments as a reference [5, 14]. As the last point, interactions between parameters were not considered since previous researchers reported that the effect of interactions between parameters were insignificant [15]. Table 2 shows simulated parameter ranges for L-PBF of Inconel 625.

Table 2. L-PBF simulation parameters for Inconel 625.

Parameter	-20%	-10%	Base Line	+10%	+20%
Laser Power (W)	228	256	285	313	342
Layer Thickness (mm)	0.032	0.036	0.04	0.044	0.048
Scanning Speed (mm/s)	768	864	960	1056	1152
Hatch Distance (mm)	0.08	0.09	0.1	0.11	0.12
Energy Density (J/mm^3)	92.77	82.47	74.22	67.47	61.85

The energy density values provided in Table 2 were calculated using Equation (1), where VED represents volumetric energy density, P represents laser power, V represents scanning speed, t represents layer thickness and h represents hatch distance.

$$\mathrm{VED} = P/(V.t.h) \quad (1)$$

3. Results and discussion

L-PBF AM process consists of a series of thermal cycles, and this cycle affects the results of the process simulations. Both the maximum heat flux and the maximum temperature values show a three-step variation in each layer. In the first step (Layer n-1.), they present extremely high values, and in the second (Layer n-2.) and third (Layer n-3.) steps they present values which are between chamber temperature (50°C) and base plate temperature (200°C). These results can be explained with the dwell which was induced with the

applied re-coater time of 9s. Fig. 2 shows the relation between process steps versus maximum heat flux and maximum temperature.

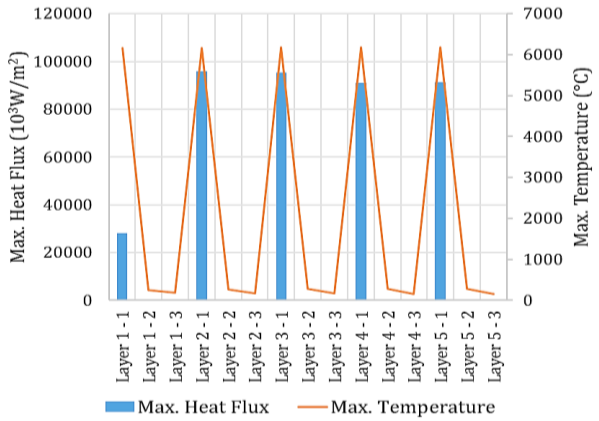

Fig 2. Process steps versus maximum heat flux and maximum temperature for the first 5 layers.

The cuboid part made of Inconel 625 alloy exhibits stresses and distortions after being exposed to thermo-mechanical effects during L-PBF AM process. The stress and distortion state of the cuboid sample varies with time. In this regard, the strain and displacement variation was observed during layer build-up and later steps such as post cooling, powder removal, unclamping, cooling and immediate release. Strains and displacements gradually increased as the result of cumulative accession. For example, the total displacement is 0.07 mm for the first layer and increases to 0.28 mm for the last. Later on, it keeps increasing to 0.41 mm at post cooling step and to 0.45 mm after immediate release from base plate as shown in Fig. 3.

On the other hand, the same straightforward trend was not applicable for effective residual stresses. Among different process steps such as layer insertion, powder re-coater time dwelling or post cooling, fluctuations were observed for the stress magnitudes. For example, while the stress magnitude for the first layer starts with 764.90 MPa, and increase to 1033.3 MPa at the last layer, it decreases again to 960.60 MPa during post cooling and reaches to 722.10 MPa after immediate release from base plate.

Fig. 3 shows the displacement and stress states of Inconel 625 cuboid during different process steps. As seen from the figure, displacements are cumulatively increasing while fluctuations exist for stress magnitude. These fluctuations can be explained by stress relaxation led by inter-layer dwell times, and accurate modeling can only be achieved with the introduction of more detailed multi-scale approaches by including temperature dependent precipitation hardening behavior of the material [16]. Just after immediate release, the cuboid part tends to show effective residual stresses trying to bend the part along build direction (+Z axis), and this leads to distortions at the tip of the cuboid. This result is compatible with the experimental findings [14].

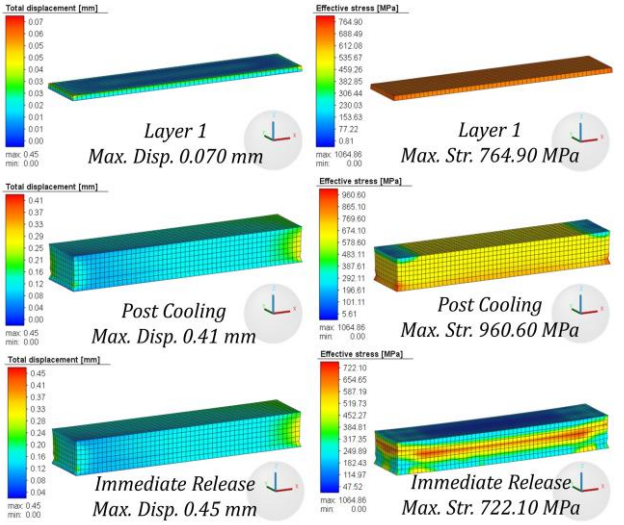

Fig 3. Displacement and stress states of Inconel 625 cuboid during different process steps.

As for the parametrical simulations, it is obvious that effective residual stresses are clearly influenced by process parameters. With the application of determined parameter set (see Table 2), the increase or decrease in the energy density altered effective residual stress results considerably. The maximum residual stress achieved was 723MPa and the minimum value was 690 MPa. Fig. 4 shows a combined graph on the influences of four main energy density parameters of laser power, layer thickness, scanning speed and hatch distance. Although all changes lead to variation of the energy density, as observed from the graph, the influence of the layer thickness was minimum while the influence of laser power and scanning speed were high. Although voxel sensitivity studies were conducted and benchmarked with experimental results in order to find to optimum voxel size, the minor influence of layer thickness could still be related to numerical underestimation. The utilized voxel size is much greater than the layer thickness. On the other hand, higher influence of laser power and scanning speed is compatible with the publications from previous literature [9, 10]. It is also interesting to examine that with the utilization of same energy density levels, laser power is much dominant in the lower side while the scanning speed has higher influence in the upper side of the optimum process parameter set. The second influential process parameter in the upper side of the optimum process parameter set is the hatch distance.

Another interesting point on the results of parametric simulations is the fact that part distortions showed negligible change although process parameters were changed, and residual stresses were influenced by these changes. The reason of the negligible changes on part distortions could be associated to bulky structure and high sectional inertia of the part geometry. Another reason could be the fact that achieved residual stress magnitudes are just below Inconel 625 material's yield strength.

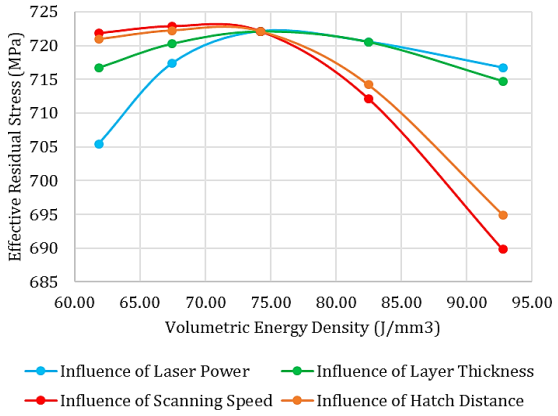

Fig 4. Influences of four main energy density parameters on residual stresses.

Finally, during the application of the parameters whose effects on the residual stresses were investigated in this study, attention should be paid to their influence on other attributes such as porosity, surface quality and form errors.

4. Conclusions

This study provides an investigation on thermo-mechanical modeling of L-PBF process of Inconel 625 alloy using Simufact Additive software. Sensitivity studies were conducted, and optimum voxel size was defined as 0.87 mm based on experimental results [14]. This value is also close to the value reported in the previous literature [15]. Parametric simulations were carried out for the energy density parameters and two dominant parameters on residual stresses were found to be the laser power and scanning speed, consistent with previous literature [9, 10]. The importance of stress relaxation led by inter-layer dwell times, and the need for multi-scale modeling approaches was emphasized as future research directions.

Acknowledgments

The authors would like to acknowledge that this study was financially supported by The Scientific And Technological Research Council Of Turkey (TÜBİTAK) in the scope of "The Analysis and Improvement of Interactions in Hybrid Manufacturing of Machining and Additive Manufacturing Technologies by Methodology Development (HyMAN)" Project (Grant No: 120M665) led by Dr. Evren Yasa.

Author's statement

Conflict of interest: Authors state no conflict of interest. Informed consent: Informed consent has been obtained from all individuals included in this study. Ethical approval: The research related to human use complies with all the relevant national regulations, institutional policies and was performed in accordance with the tenets of the Helsinki Declaration, and has been approved by the authors' institutional review board or equivalent committee.

References

1. ASTM International. ISO/ASTM52900-15 Standard Terminology for Additive Manufacturing – General Principles – Terminology. West Conshohocken, PA; ASTM International, 2015. doi: https://doi.org/10.1520/ISOASTM52900-15
2. ASTM International. ISO/ASTM52911-1-19 Additive manufacturing — Design — Part 1: Laser-based powder bed fusion of metals. West Conshohocken, PA; ASTM International, 2019. doi: https://doi.org/10.1520/F3280-19
3. Özsoy, K., Duman, B., and D.İ. Gültekin, Metal part production with additive manufacturing for aerospace and defense industry. Uluslararası Teknolojik Bilimler Dergisi, 2019. 11.3: p. 201-210.
4. Kuşhan, M. C., Poyraz, Ö., Uzunonat, Y., and S. Orak, Systematical review on the numerical simulations of laser powder bed additive manufacturing. Sigma: Journal of Engineering & Natural Sciences/Mühendislik ve Fen Bilimleri Dergisi, 2018. 36(4): p. 1197-1212.
5. Yasa, E. and O. Poyraz, Investigation of residual stresses by micro indentation in selective laser melting. Journal of The Faculty of Engineering and Architecture of Gazi University, 2021. 36 (2): p. 1029-1039. doi: https://doi.org/10.17341/gazimmfd.792584
6. Khan, H. M., et al., Influence of the post-processing operations on surface integrity of metal components produced by laser powder bed fusion additive manufacturing: a review. Machining Science and Technology, 2020, 25 (1): p. 118-17. doi: https://doi.org/10.1080/10910344.2020.1855649
7. Peter, N., et al., Benchmarking build simulation software for laser powder bed fusion of metals. Additive Manufacturing, 2020. 36, 101531: p. 1-23. doi: https://doi.org/10.1016/j.addma.2020.101531
8. Çelebi, A. and E. Z. Appavuravther, Analyzing the Effect of Voxel-Based Surface Mesh Application on Residual Stress with Simufact Additive Software. Düzce University Journal of Science & Technology, 2018. 6: p. 930-940. doi:
9. Huo, Y. S., et al, Influence of different Processing Parameter on distortion and Residual Stress of Inconel 718 Alloys Fabricated by Selective Laser Melting (SLM). Materials Research, 2020. 23(6): p. 1-7. doi: https://doi.org/10.1590/1980-5373-MR-2020-0176
10. Şirin, T. B. and Y. Kaynak, Prediction of residual stress and distortion in laser powder bed fusion additive manufacturing process of Inconel 718 alloy. Procedia CIRP, 2021. 99: p. 330-335. doi: https://doi.org/10.1016/j.procir.2021.03.102
11. Donachie, M. J. and S.J. Donachie, Superalloys: a technical guide. ASM international, 2002.
12. ASTM International. F3056-14e1 Standard Specification for Additive Manufacturing Nickel Alloy (UNS N06625) with Powder Bed Fusion. West Conshohocken, PA; ASTM International, 2014. doi: https://doi.org/10.1520/F3056-14E01
13. MSC Software Corporation, Introducing Simufact Additive in Simufact Additive Tutorial. Simufact Additive GmbH, 2018.
14. Kundakçıoğlu, E, Modeling of temperature field, residual stresses and distortions in direct laser metal sintering. PhD Thesis, Graduate School of Engineering, Koç University, İstanbul, Turkey, 2019.
15. Bastus, A. M, Numerical sensitivity study of residual stress and distortion in selective laser melting of 17-4 PH steel, Master's Thesis, Chair of Mechanical Engineering, Montanuniversität Leoben, Austria, 2019.
16. Denlinger, E. R. and P. Michaleris, Effect of stress relaxation on distortion in additive manufacturing process modeling, Additive Manufacturing, 2016. 12: p. 51-59, doi: https://doi.org/10.1016/j.addma.2016.06.011

17. Bugatti, M., and Q. Semeraro, Limitations of the inherent strain method in simulating powder bed fusion processes, Additive Manufacturing, 2018. 23: p. 329-346. https://doi.org/10.1016/j.addma.2018.05.041
18. Cheng, L. and A. To, Part-scale build orientation optimization for minimizing residual stress and support volume for metal additive manufacturing: Theory and experimental validation. Computer-Aided Design, 2019 113: p. 1-23. https://doi.org/10.1016/j.cad.2019.03.004